Mon. Not. R. Astron. Soc. **000**, 000–000 (0000) Printed 30 August 2016 (MN LATEX style file v2.2)

Concise estimate of the expected number of detections for stellar-mass binary black holes by eLISA

Koutarou Kyutoku[1] and Naoki Seto[2]
[1] *Interdisciplinary Theoretical Science (iTHES) Research Group, RIKEN, Wako, Saitama 351-0198, Japan*
[2] *Department of Physics, Kyoto University, Kyoto 606-8502, Japan*

arXiv:1606.02298v2 [astro-ph.HE] 29 Aug 2016

30 August 2016

ABSTRACT

We study prospects for detecting extragalactic binary black holes similar to GW150914 by evolved Laser Interferometer Space Antenna (eLISA). We find that the majority of detected binary black holes will not merge within reasonable observation periods of eLISA in any configuration. While long-arm detectors are highly desired for promoting multiband gravitational-wave astronomy by increasing the detections of merging binaries, the number of total detections can be increased also by improving the acceleration noise. A monochromatic approximation works well to derive semiquantitative features of observational prospects for non-merging binaries with clearly indicating the parameter dependence. Our estimate also suggests that the number of galaxies in the error volume is so small that the host galaxy may be determined uniquely with high confidence.

Key words: gravitational waves — binaries: close

1 INTRODUCTION

The first detection of a binary-black hole merger, GW150914, opened the door to gravitational-wave astronomy (Abbott et al. 2016a). The masses of the black holes, ~ 29 and $\sim 36M_\odot$, are larger than ~ 10–$15M_\odot$ previously expected from galactic observations (Özel et al. 2010; Kreidberg et al. 2012), and this finding prompts a vigorous debate regarding their origin. At the same time, Abbott et al. (2016c) suggest a very high merger rate of binary black holes in our Universe based on a part of Advanced LIGO's O1 observation run. These facts immediately mean that space-based gravitational-wave detectors, such as evolved Laser Interferometric Space Antenna (eLISA: see Armano et al. 2016, for LISA Pathfinder), would have a fair chance to detect extragalactic stellar-mass binary black holes as well as galactic compact binaries (Abbott et al. 2016b; Sesana 2016).

Observing gravitational waves at low frequency will be important to understand the origin of massive black holes like GW150914. Facing massive black holes with $\gtrsim 30M_\odot$ unexpected for end products of stellar evolution with the solar metallicity (Abbott et al. 2016b), possible formation channels of the binary are actively discussed. One plausible scenario is the evolution of low-metallicity stars with weak stellar winds in an isolated field binary (see Postnov & Yungelson 2014, for reviews). Another scenario is dynamical formation in dense stellar environments like galactic nuclei or globular clusters (see, e.g., Benacquista & Downing 2013; Rodriguez et al. 2015, 2016). It is also pointed out that a binary of primordial black holes satisfying current observational constraints is also consistent with GW150914 (Bird et al. 2016; Sasaki et al. 2016). Because these scenarios predict different distribution of binary parameters such as the eccentricity, which is determined to higher accuracy at lower frequency (see section 1 of Nishizawa et al. 2016b, for the discussion), multiple detections could statistically clarify the formation scenario (see also Breivik et al. 2016; Nishizawa et al. 2016a). Moreover, precise localization of the binary by the annual modulation of the detector with the distance estimation will be beneficial to determine the host galaxy, information of which is also invaluable to infer the origin.

In this paper, we study prospects for detecting extragalactic binary black holes by eLISA, enhancing the previous investigation for Galactic binary black holes by one of the authors (Seto 2016). The possibility of detecting extragalactic binary black holes is mentioned briefly by LIGO Scientific Collaboration immediately after the detection of GW150914 (Abbott et al. 2016b). Various authors conducted follow-up studies of this possibility by Monte Carlo simulations (Nishizawa et al. 2016b; Sesana 2016; Vitale 2016), primarily focusing on the aspects of multiband gravitational-wave astronomy, i.e., simultaneous detections of the same binary by eLISA and ground-based interferometric detectors such as Advanced LIGO. Here, we analytically evaluate the expected number of detections and put more emphasis on extragalactic binary black holes that do not merge during the operation of eLISA than previous studies do, because such

© 0000 RAS

binaries inevitably dominate the detection. We also show that a monochromatic approximation works well to derive semiquantitative features of observational prospects for nonmerging binaries.

Our assumptions and parameter choices are summarized as follows. We treat all the binary black holes as circular, and denote the gravitational-wave frequency by f, which is twice the orbital frequency. This is justified to the accuracy of our discussion, because the eccentricity is not expected to be very high. We apply the quadrupole formula for point masses neglecting the black hole spin as well as higher order post-Newtonian effects, and the cosmological redshift is also neglected. We take the fiducial chirp mass of binary black holes to be $\mathcal{M} = 28M_\odot$ according to the estimate from GW150914 (Abbott et al. 2016a), and later show that our estimate applies approximately to distribution of chirp masses once averaged over the weight $\mathcal{M}^{10/3}$. We take the fiducial comoving merger rate to be $R = 100\,\mathrm{Gpc}^{-3}\,\mathrm{yr}^{-1}$ motivated by the estimate from a part of O1 (Abbott et al. 2016c).

2 SEARCH FOR EXTRAGALACTIC BINARY BLACK HOLES

In this section, we derive the frequency distribution of the expected number of detections for extragalactic binary black holes by eLISA with various planned sensitivities. We take the fiducial value of the observation period T to be 3 yr in the same manner as Seto (2016) and the fiducial value of the detection threshold for the signal-to-noise ratio $\rho_{\rm thr}$ to be 8.

2.1 formulation

The signal-to-noise ratio ρ for a binary with the initial frequency f_i at the start of the observation is given by

$$\rho^2 = 4\int_{f_i}^{f_f} \frac{|\tilde{h}(f)|^2}{(3/20)S(f)}df, \tag{1}$$

where $S(f)$ is the one-sided, sky-averaged noise spectral density of eLISA such as those provided in Amaro-Seoane et al. (2012); Klein et al. (2016). The factor of 3/20 is introduced to derive an effective non-sky-averaged noise spectral density (Berti, Buonanno & Will 2005; Nishizawa et al. 2016b). The frequency f_f at the end of the observation is given by

$$f_f(f_i, T) = \left(f_i^{-8/3} - \frac{256\pi^{8/3}G^{5/3}\mathcal{M}^{5/3}T}{5c^5}\right)^{-3/8}, \tag{2}$$

as long as the binary does not merge within the observation period. The frequency above which the merger occurs within the observation period T is given by

$$f_{\rm merge}(T) = \frac{5^{3/8}c^{15/8}}{8\pi G^{5/8}\mathcal{M}^{5/8}T^{3/8}} \tag{3}$$

$$= 19.2\,\mathrm{mHz}\left(\frac{\mathcal{M}}{28M_\odot}\right)^{-5/8}\left(\frac{T}{3\,\mathrm{yr}}\right)^{-3/8}, \tag{4}$$

and such binaries will serve as interesting targets of multiband gravitational-wave astronomy (Sesana 2016; Vitale 2016; Nishizawa et al. 2016b). If the binary merges within the observation period, namely $f_i \geqslant f_{\rm merge}(T)$, or f_f becomes higher than 1 Hz, above which the detector noise would lose control, we set f_f in equation (1) to be 1 Hz.

The gravitational-wave spectral amplitude for a binary at a distance D is given by

$$\left|\tilde{h}(f)\right|^2 = \frac{5G^{5/3}\mathcal{M}^{5/3}}{24\pi^{4/3}c^3D^2f^{7/3}} \times \frac{3}{4}\left[F_+^2\left(\frac{1+\mu^2}{2}\right)^2 + F_\times^2\mu^2\right], \tag{5}$$

where F_+ and $F_\times$ are the antenna pattern functions, which depend on the sky location and polarization angle, and $\mu = \cos\imath$ is the cosine of the inclination angle $\imath$. We explicitly separate the factor $(\sqrt{3}/2)^2$ accounting the opening angle 60° of eLISA from the antenna pattern functions. The antenna pattern functions also change with time due to the annual rotation of the detector plane.

Because we focus on the case that $T \geqslant 1\,\mathrm{yr}$, we take the time average of the antenna pattern functions in advance to set $\langle F_+^2\rangle_t = \langle F_\times^2\rangle_t = 1/5$ for individual binaries. This is a reasonable approximation at least for a six-link configuration (Seto 2004).[1] Meanwhile, even for a four-link configuration, we can extend the procedure developed in Seto (2014) to show that the averaging with respect to the polarization angle has a negligible effect of $\sim 1\%$ level on the detectable volume $V(f_i, T)$ estimated below. We assume a four-link configuration of eLISA in this study, and the result for a six-link configuration may be estimated simply multiplying $\tilde{h}(f)$ by a factor of $\sqrt{2}$ and scaling all the relevant quantities accordingly.

Then, the signal-to-noise ratio relevant for our study is expressed as

$$\rho^2 = \frac{A^2}{D^2}\left[\left(\frac{1+\mu^2}{2}\right)^2 + \mu^2\right] I_7(f_i, T), \tag{6}$$

$$A^2 \equiv \frac{G^{5/3}\mathcal{M}^{5/3}}{8\pi^{4/3}c^3}, \tag{7}$$

$$I_7(f_i, T) \equiv \int_{f_i}^{f_f} \frac{f^{-7/3}}{(3/20)S(f)}df. \tag{8}$$

Note that I_7 defined above depends on the initial frequency f_i and the observation period T. The maximum detectable distance within which the signal-to-noise ratio is larger than a given threshold $\rho_{\rm thr}$ depends on the inclination angle, initial frequency, and observation period as

$$D_{\rm thr} = \frac{A}{\rho_{\rm thr}}\left[\left(\frac{1+\mu^2}{2}\right)^2 + \mu^2\right]^{1/2} I_7(f_i, T)^{1/2}. \tag{9}$$

The detectable volume averaged over the inclination angle becomes a function of the initial frequency and observation period as

$$V(f_i, T) = \frac{4\pi}{3} \times \frac{1}{2}\int_{-1}^{1} D_{\rm thr}^3 d\mu, \tag{10}$$

and the effective range (or sensemon range) of eLISA is also

[1] For a binary with a short signal duration, the average over the sky location is less than 0.221. Given the convex nature of the function $x^{3/2}$ that relates the signal-to-noise ratio and the effective volume, the actual value should be in the range $[0.2, 0.221]$, resulting in an error less than 17% for our effective volume below.

defined by $D_{\rm eff} \equiv (3V/4\pi)^{1/3}$. Using (see also Schutz 2011)

$$\frac{1}{2}\int_{-1}^{1}\left[\left(\frac{1+\mu^2}{2}\right)^2+\mu^2\right]^{3/2} d\mu \approx 0.822, \tag{11}$$

the detectable volume averaged over the inclination angle is calculated as

$$V(f_i,T) = \frac{4\pi}{3}\times 0.822\frac{A^3}{\rho_{\rm thr}^3} I_7(f_i,T)^{3/2}, \tag{12}$$

and the effective range is given by

$$D_{\rm eff}(f_i,T) = 0.937\frac{A}{\rho_{\rm thr}} I_7(f_i,T)^{1/2}. \tag{13}$$

Hereafter, we denote the initial frequency simply by f anticipating no confusion would arise.

The frequency distribution of the expected number of detections for binary black holes can be calculated as

$$\frac{dN}{d\ln f} = V(f,T)\frac{dn}{d\ln f}, \tag{14}$$

where $dn/d\ln f$ is the number-density distribution of the binaries. For a collection of identical binary black holes, the distribution of the number density n in each logarithmic frequency interval should be proportional to the time that binaries spend in the interval. Here, we specifically consider the collection of binary black holes similar to GW150914. Using the comoving merger rate $R = dn/dt$, the distribution is written as

$$\frac{dn}{d\ln f} = \frac{f}{\dot f}R = \frac{5c^5 R}{96\pi^{8/3}G^{5/3}\mathcal{M}^{5/3}f^{8/3}} \tag{15}$$

$$= 4.57\times 10^{-6}\,{\rm Mpc}^{-3} \times\left(\frac{f}{10\,{\rm mHz}}\right)^{-8/3}\left(\frac{\mathcal{M}}{28M_\odot}\right)^{-5/3}\left(\frac{R}{100\,{\rm Gpc}^{-3}\,{\rm yr}^{-1}}\right). \tag{16}$$

The distribution of the expected number of detections, $dN/d\ln f$, is obtained by multiplying equations (12) and (15), where it is proportional to $R/\rho_{\rm thr}^3$ as expected. The distance $D_{\rm near}$ to the nearest and thus loudest binary black holes in each logarithmic frequency interval can be guessed from this number-density distribution via the condition

$$\frac{4\pi}{3}D_{\rm near}^3(f)\frac{dn}{d\ln f} = 1, \tag{17}$$

and it is found to be

$$D_{\rm near}(f) = \frac{3^{2/3}2\pi^{5/9}G^{5/9}\mathcal{M}^{5/9}f^{8/9}}{5^{1/3}c^{5/3}R^{1/3}} \tag{18}$$

$$= 37.4\,{\rm Mpc} \times\left(\frac{f}{10\,{\rm mHz}}\right)^{8/9}\left(\frac{\mathcal{M}}{28M_\odot}\right)^{5/9}\left(\frac{R}{100\,{\rm Gpc}^{-3}\,{\rm yr}^{-1}}\right)^{-1/3}. \tag{19}$$

To indicate the relevant distance scale of the problem, we show the effective range $D_{\rm eff}(f)$ for two representative noise curve models of eLISA (Amaro-Seoane et al. 2012; Klein et al. 2016) and the distance to the nearest binary $D_{\rm near}(f)$ in Fig. 1. This figure shows that the relevant range is local with $\lesssim 350$ Mpc. The expected number of detections becomes lower than unity for the frequency range

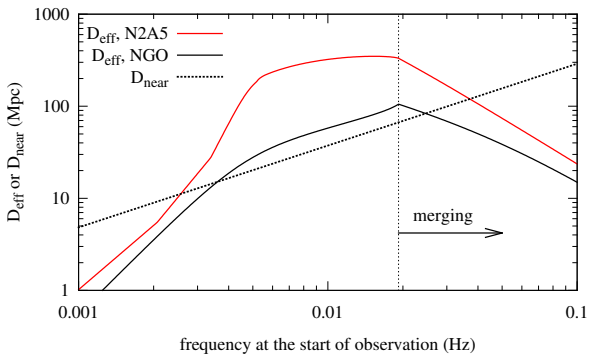

Figure 1. Effective range $D_{\rm eff}$ for 3-yr observations of eLISA and the distance $D_{\rm near}$ to the nearest binary black holes similar to GW150914. The curves for $D_{\rm eff}$ labelled by NGO and N2A5 are calculated with the noise curve of Amaro-Seoane et al. (2012) and that of Klein et al. (2016), respectively. Galactic binary white dwarfs are taken into account as the foreground for the latter according to Klein et al. (2016). The vertical dotted line marks $f_{\rm merge}(3\,{\rm yr}) = 19.2\,{\rm mHz}$.

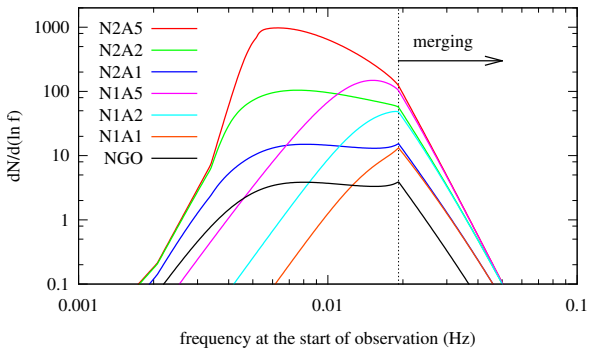

Figure 2. Frequency distribution of the expected number of detections for binary black holes similar to GW150914 in each logarithmic frequency interval for 3-yr observations of eLISA. The curve labeled by NGO is calculated with the noise curve of Amaro-Seoane et al. (2012), and the others are with those of Klein et al. (2016). Galactic binary white dwarfs are taken into account as the foreground for N2 configurations according to Klein et al. (2016). The vertical dotted line marks $f_{\rm merge}(3\,{\rm yr}) = 19.2\,{\rm mHz}$.

where $D_{\rm eff} \lesssim D_{\rm near}$, and thus the actual number will fluctuate significantly. This fluctuation will especially be relevant for the detection of merging binary black holes satisfying $f > f_{\rm merge}(T)$ by low-sensitivity configurations such as NGO (Amaro-Seoane et al. 2012), with which $D_{\rm eff}/D_{\rm near}$ never exceeds 2 irrespective of the frequency.

2.2 Frequency distribution of the expected number of detections

Fig. 2 shows the distribution, $dN/d\ln f$ (equation 14), calculated with various noise curve models of eLISA (Amaro-Seoane et al. 2012; Klein et al. 2016). For models of Klein et al. (2016), N2 has a weaker acceleration noise than N1, and the sensitivity is improved primarily at low frequency. A1, A2, and A5 correspond to the arm length of 1×10^6 km,

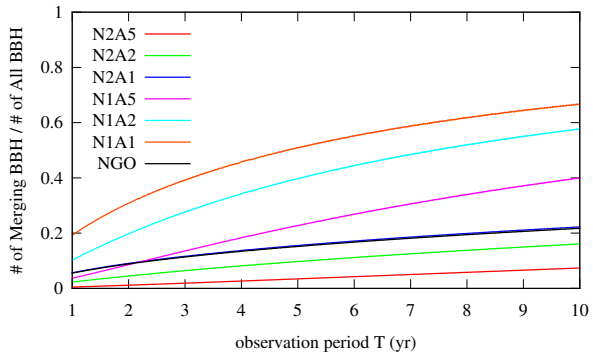

Figure 3. Fraction of detected binary black holes that merge within the observation period of eLISA to all the detected binary black holes as a function of the observation period. The curve for N2A1 mostly overlaps with that for NGO due to the similar shape of the noise curve.

2×10^6 km, and 5×10^6 km, respectively, and the long arm length improves the sensitivity at intermediate frequency.

This figure shows that the noise curve has a critical impact on the number of detections and also that the majority of the detected binaries will not merge within the observation period in any case. The number of merging binary black holes satisfying $f \geqslant f_{\rm merge}(T)$ is not affected significantly by the sensitivity at low frequency, as found from the comparisons between N1 and N2 configurations. This is expected, because additional detections of merging binary black holes require improvement of the sensitivity at $f \geqslant f_{\rm merge}(T)$. On another front, a long arm length increases the detections of merging binary black holes significantly, as found from the comparisons among A1, A2, and A5 configurations. Both improvements enhance the number of total detections.

The dominance of non-merging binary black holes is always the case for reasonable observation periods as shown in Fig. 3. This figure shows that merging binary black holes become dominant only for an improbably long observational period of $T \gtrsim 5\,$yr with the N1 configurations, which are less sensitive at low frequency (see also Sesana 2016). The fraction will be no larger than $\sim 10\%$ for the N2 configurations because of its high sensitivity at low frequency, which drastically increases the detections of non-merging binary black holes. The fraction is nearly the same for NGO and N2A1, because they have very similar noise curves except for the overall normalization.

The number of merging binary black holes itself is always larger for the N2 configurations than the N1 configurations as well as that of all the detected binary black holes as shown in Fig. 4. We also present the numbers for representative values of T in Table 1. This figure shows that the number of detections for extragalactic stellar-mass binary black holes could be comparable to that for supermassive binary black holes (Klein et al. 2016). This figure also shows that the number of (merging or total) detected binaries increases faster than the increase of the observation period, T. As we explain in the next section, the total number is expected to increase approximately as $T^{3/2}$ for the case that dominant sources do not evolve significantly, i.e., the monochromatic approximation applies well. This is the case for eLISA. This situation should be contrasted with compact

Table 1. The expected number of all the detected binary black holes and merging binary black holes for representative values of the observation period, T.

Model	1 yr	2 yr	3 yr	4 yr	5 yr	10 yr
NGO	1.2	3.4	6.2	9.5	13.2	36.2
(merge)	0.07	0.3	0.7	1.3	2.0	7.9
N1A1	1.4	3.7	6.5	9.6	13.0	32.3
(merge)	0.3	1.1	2.5	4.4	6.6	21.6
N1A2	6.0	16.5	29.5	44.3	60.3	153
(merge)	0.6	3.3	8.1	15.2	23.9	88.8
N1A5	22.2	61.9	112	170	235	621
(merge)	0.8	5.3	15.1	31.2	53.2	249
N2A1	4.7	13.2	24.0	36.6	50.8	139
(merge)	0.3	1.2	2.8	5.0	7.9	31.0
N2A2	27.6	77.6	142	217	302	835
(merge)	0.6	3.5	9.1	17.7	29.2	135
N2A5	174	492	903	1390	1940	5420
(merge)	0.8	5.7	17.0	36.9	66.3	401

binary coalescences for ground-based detectors, the number of which should be proportional to T. In reality, the increase could be even faster for eLISA, because the long-term observation will allow us to remove more confusion noise caused by Galactic compact binaries. The total expected number of detections varies by two orders of magnitude, from ~ 6 (NGO) to ~ 900 (N2A5) for $T = 3\,$yr, among different detector configurations.

The prospect for multiband gravitational-wave astronomy crucially depends on the detector arm length. If the arm length is $\sim 1 \times 10^6$ km (A1), the number of binaries that merge within the observation period is $O(1)$ at best. Even if we would count binaries that merge within $\sim 10\,$yr after the shutdown of eLISA, the number will be only $\lesssim 30$. By contrast, the arm length of $\sim 5 \times 10^6$ km (A5) would increase the number of merging binary black holes by a factor of several. Thus, the long arm length of eLISA is highly desired for fruitful multiband gravitational-wave astronomy. Reducing the acceleration noise adds not much to multiband observations. Our estimates agree approximately with those of Sesana (2016) derived by Monte Carlo simulations with distribution of chirp masses.

3 MONOCHROMATIC APPROXIMATION

In the low-frequency regime where the binary evolution is negligible during the observation period, the monochromatic approximation works well to estimate various aspects of detectable signals. The signal-to-noise ratio of gravitational waves is approximated by

$$\rho^2 \approx 4 \frac{|\tilde{h}(f)|^2}{(3/20)S(f)} \dot{f} T \tag{20}$$

$$= \frac{12\pi^{4/3} G^{10/3} \mathcal{M}^{10/3}}{5c^8 D^2} \left[\left(\frac{1+\mu^2}{2} \right)^2 + \mu^2 \right] \frac{f^{4/3} T}{(3/20)S(f)}, \tag{21}$$

where the time and polarization angle average are assumed. After averaging over the inclination angle, the frequency distribution of the expected number of detections becomes

$$\frac{dN}{d\ln f} \approx 0.822 \times \frac{\pi^{1/3} G^{10/3} \mathcal{M}^{10/3} R}{3^{1/2} 5^{1/2} c^7 \rho_{\rm thr}^3} \frac{f^{-2/3} T^{3/2}}{[(3/20)S(f)]^{3/2}} \tag{22}$$

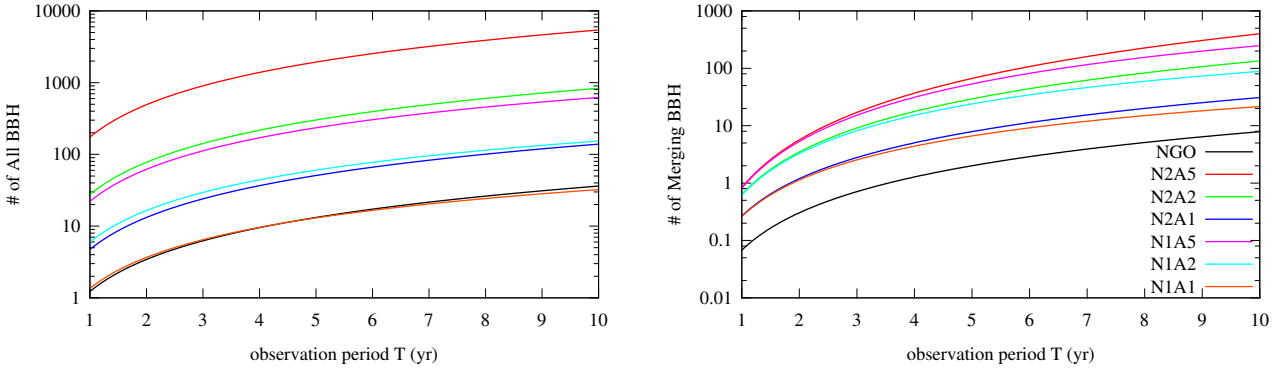

Figure 4. Expected number of all the detected binary black holes (left) and merging binary black holes (right) as functions of the observation period of eLISA. Note the different scale of the vertical axes.

in the monochromatic approximation.

A remarkable point is that the expected number of detections is proportional to $\mathcal{M}^{10/3}$. This expression implies that our simple estimate should also be valid approximately for the case that the chirp mass has distribution, once we replace $\mathcal{M}$ by the averaged chirp mass defined by

$$\langle \mathcal{M} \rangle \equiv \left[\int p(\mathcal{M}) \mathcal{M}^{10/3} d\mathcal{M} \right]^{3/10}, \qquad (23)$$

where $p(\mathcal{M})$ is the probability distribution of the chirp mass. For example, if the realistic typical chirp mass would be $\sim 9 M_\odot$ corresponding to a $10 M_\odot$–$10 M_\odot$ binary, the number of detections is smaller by a factor of $\sim$ 40–50 than the current estimate. This dependence should be compared with $\mathcal{M}^{5/2}$ expected for ground-based detectors (see equations 6 and 7), which observe chirping signals.

The distribution scales as $\propto T^{3/2}$ because of the relation $\rho \propto T^{1/2}$. This means that a longer operation of eLISA will detect more binary black holes than the increase linear in time differently from compact binary coalescences for ground-based detectors. The longer operation will further increase the detections of non-merging binary black holes by removing more confusion noise caused by Galactic compact binaries, and thus $T^{3/2}$ is conservative. While this effect will not be relevant to merging binary black holes at high frequency, their detections should also increase even faster than $T^{3/2}$, because the longer operation of eLISA allows binaries at lower frequency to merge within the observation period.

Fig. 5 compares $dN/d\ln f$ obtained by the exact integration, equation (14), and that by the monochromatic approximation, equation (22), for $T = 3\,\mathrm{yr}$. The agreement is quite good at frequency lower than $f_{\rm merge}(T)$, particularly for N2A5. The deviation is only by a factor of less than 2 at $f_{\rm merge}(T)$ even for NGO. This clearly shows that the monochromatic approximation works quite well to estimate the number of non-merging binary black holes. By contrast, the monochromatic approximation significantly overestimates the number of merging binary black holes at high frequency. The breakdown of this approximation at $f \gtrsim f_{\rm merge}(T)$ is inevitable, because the binary evolution necessarily becomes important. Still, taking the fact that the detections is dominated by non-merging binaries, the monochromatic approximation is useful to derive semiquantitative dependence of characteristic quantities on relevant parameters and to evaluate detector performance by a concise calculation.

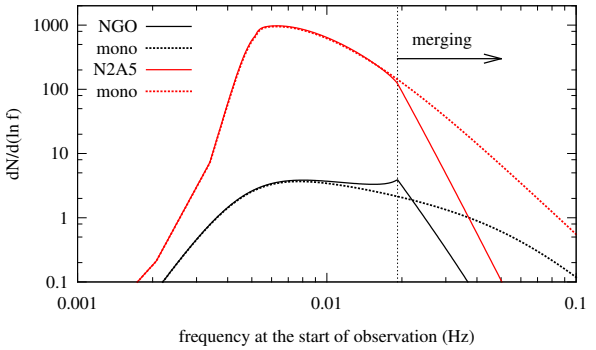

Figure 5. Comparison of the frequency distribution of the expected number of detections obtained by the exact expression, equation (14) (solid curve), and that by the monochromatic approximation, equation (22) (dashed curve). The results for NGO (black) and N2A5 (red) configurations are shown assuming 3-yr observations. The vertical dotted line marks $f_{\rm merge}(3\,\mathrm{yr}) = 19.2\,\mathrm{mHz}$.

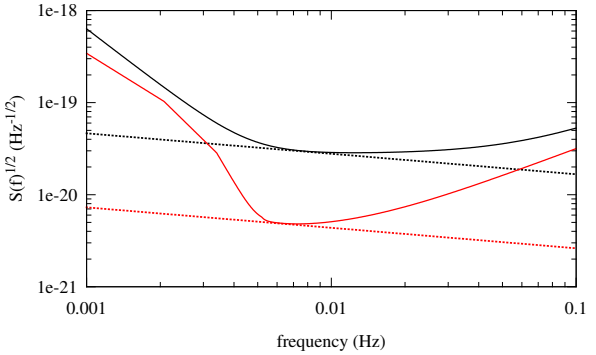

Figure 6. Tangential line with the slope $-2/9$ to the square root of $S(f)$. The black and red curves are for NGO and N2A5, respectively.

The frequency at which the distribution, $dN/d\ln f$, peaks will dominate the detections, and it can be evaluated graphically by drawing a tangential line with an appropriate slope to the noise spectral density. Specifically, equation (22)

shows that the peak frequency is obtained as a contact point of a tangential line with the slope $-2/9$, i.e., $\propto f^{-2/9}$, to the square root of the noise spectral density, $S(f)^{1/2}$, as shown in Fig. 6. The same can be done by taking the minimum of $S(f)f^{4/9}$.

4 LOCALIZATION ERROR

We briefly estimate the localization error using empirical formulae derived in Takahashi & Seto (2002) adopting the monochromatic approximation and Fisher analysis (see also Cutler 1998; Vecchio & Wickham 2004). The errors of the sky location and the distance to the source for $T \gtrsim 2\,\mathrm{yr}$ are, respectively, given by (recall $1\,\mathrm{deg}^2 = 3.0 \times 10^{-4}\,\mathrm{str}$)

$$\Delta\Omega(f) \sim 7.1 \times 10^{-4}\,\mathrm{str} \left(\frac{\rho}{10}\right)^{-2} \left(\frac{f}{10\,\mathrm{mHz}}\right)^{-2}, \tag{24}$$

$$\frac{\Delta D}{D} \sim 0.2 \left(\frac{\rho}{10}\right)^{-1}. \tag{25}$$

Here, the empirical formula of $\Delta\Omega(f)$ is applicable to $f \gtrsim 2\,\mathrm{mHz}$ where the source is localized primarily by the Doppler shift associated with the annual motion of the detector (Takahashi & Seto 2002). Thus, the formula is appropriate for the frequency range that we are interested in this study (see Fig. 1). Assuming the error volume ΔV to have an elliptical shape in conformity with the Fisher analysis, we find

$$\Delta V(f) \sim \frac{4}{3} D^2 \Delta\Omega(f) \Delta D \tag{26}$$

$$\sim 200\,\mathrm{Mpc}^3 \left(\frac{D}{100\,\mathrm{Mpc}}\right)^3 \left(\frac{\rho}{10}\right)^{-3} \left(\frac{f}{10\,\mathrm{mHz}}\right)^{-2}. \tag{27}$$

While this expression is valid for any monochromatic source, the signal-to-noise ratio, ρ, is determined by D and f for binary black holes with given binary parameters such as the chirp mass and the inclination angle.

In this section, we focus on the nearest and thus loudest binaries located at $D_{\mathrm{near}}(f)$, because the error volume should be the smallest for such systems and the host galaxy should be determined most accurately. To derive the signal-to-noise ratio, we average the inclination angle somewhat arbitrarily in the same manner as is done in the previous section, equation (11). This averaging has a useful feature that the signal-to-noise ratio for the nearest binary becomes $\rho_{\mathrm{thr}} D_{\mathrm{eff}}/D_{\mathrm{near}}$. The error volume for the nearest binary $(\Delta V)_{\mathrm{near}}$ is found to be proportional to $D_{\mathrm{near}}^6 D_{\mathrm{eff}}^{-3} f^{-2}$ irrespective of the precise averaging procedure, and furthermore in the monochromatic approximation, proportional to $f^{4/3} S(f)^{3/2}$. This implies that the smallest error volume is achieved at the minimum of $S(f)f^{8/9}$ or equivalently the contact point of $S(f)^{1/2}$ and a tangential line with the slope $-4/9$. For eLISA noise curves, the minimum of $(\Delta V)_{\mathrm{near}}$ is very close to the maximum of $dN/d\ln f$.

Fig. 7 shows the error volume for the nearest and thus loudest binaries in each logarithmic frequency interval. This figure is drawn using the exact integration, equation (14), rather than the monochromatic approximation, equation (22), and the results are nearly identical below $f_{\mathrm{merge}}(T)$. Assuming the typical number density of galaxies $\sim 0.01\,\mathrm{Mpc}^{-3}$, this figure strongly suggests that we may be

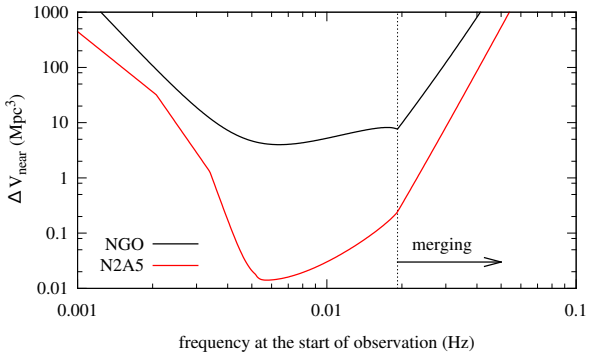

Figure 7. Error volume $\Delta V(f)$ for the nearest and thus loudest binaries located at $D_{\mathrm{near}}(f)$ for 3-yr observations of eLISA. The black and red curves are for NGO and N2A5, respectively. It should be cautioned that the result below $\sim 2\,\mathrm{mHz}$ is poorly described by the empirical formula adopted in this study, equation (24). The vertical dotted line marks $f_{\mathrm{merge}}(3\,\mathrm{yr}) = 19.2\,\mathrm{mHz}$.

able to determine the host galaxy of many binary black holes with very high confidence. Because massive binary black holes like GW150914 are hardly expected to be localized accurately by ground-based detectors, which crucially rely on high-frequency signals with $f \gtrsim 100\,\mathrm{Hz}$ via the triangulation (Fairhurst 2009), the exquisite accuracy of localization by eLISA will be invaluable to study the origin of massive binary black holes. The accurate determination of the host galaxy will also be important to study the cosmology using binary black holes as standard sirens (Schutz 1986).

Our estimate refers only to the statistical error. Taking the high precision of localization by eLISA, other sources of errors such as the inaccuracy of templates would require serious consideration (Cutler & Vallisneri 2007). Furthermore, the error volume estimated above is not accurate at high frequency, because the monochromatic approximation used to derive equation (27) breaks down. The estimate for $f \lesssim 2\,\mathrm{mHz}$ is also inaccurate, because the empirical formula does not apply. While the statistical error in the frequency range where most of the binaries are detected is handled properly in our discussion, it would be interesting to study the localization error in a more comprehensive manner along the line of our concise calculation to complement Monte Carlo simulations (Nishizawa et al. 2016b; Sesana 2016; Vitale 2016). In addition, the eccentricity estimation will also be important to clarify the nature of massive binary black holes, and thus it would be useful to assess the estimation error in a quantitative manner. The eccentricity may be estimated via the amplitude of the third harmonic mode in the monochromatic limit (Seto 2016) or via the matched-filtering analysis at high frequency, for which Nishizawa et al. (2016b) gave error distribution by Monte Carlo simulations combined with the Fisher analysis. We left such extension for the future study.

5 SUMMARY

We investigate the prospects for detecting extragalactic stellar-mass binary black holes by eLISA, motivated by the first direct detection of gravitational waves, GW150914. eLISA might observe as many binary black holes similar to

GW150914 as supermassive binary black holes. The detection will be dominated by binaries that do not merge within the observation period T of eLISA, particularly when the low-frequency acceleration noise is improved. The total number of detections varies by about two orders of magnitude depending on the detector sensitivity, and a long-arm detector is highly desired for promoting multiband gravitational-wave astronomy by increasing the detections of merging binary black holes. Scientific returns from a long operation is more than the increase linear in time. Specifically, the total number of detections increases as or faster than $T^{3/2}$, and the number of merging binary black holes increases much faster than $T^{3/2}$.

A monochromatic approximation works well to derive various features of observational prospects, especially for the case that the sensitivity is high at low frequency so that the detections of non-merging binary black holes are numerous. The expected number of detections is found to be proportional to $\mathcal{M}^{10/3}$ by the monochromatic approximation, and our estimate will be applicable to binary black holes with chirp-mass distribution if we use the appropriately weighted average chirp mass (equation 23). The error volume of the localization can be so small that the host galaxy is determined with high confidence. This ability of eLISA will be invaluable to clarify the origin of massive binary black holes.

ACKNOWLEDGEMENTS

This work is supported by JSPS Kakenhi Grant-in-Aid for Research Activity Start-up (No. 15H06857), for Scientific Research (No. 15K65075) and for Scientific Research on Innovative Areas (No. 24103006). Koutarou Kyutoku is supported by the RIKEN iTHES project.

REFERENCES

Abbott B. P. et al., 2016a, Phys. Rev. Lett., 116, 061102
Abbott B. P. et al., 2016b, Astrophys. J., 818, L22
Abbott B. P. et al., 2016c, arXiv:1602.03842
Amaro-Seoane P. et al., 2012, Classical Quantum Gravity, 29, 124016
Armano M. et al., 2016, Phys. Rev. Lett., 116, 231101
Benacquista M. J., Downing J. M. B., 2013, Living Rev. Relativity, 16, 4
Berti E., Buonanno A., Will C. M., 2005, Phys. Rev. D, 71, 084025
Bird S., Cholis I., Muñoz J. B., Ali-Haïmoud Y., Kamionkowski M., Kovetz E. D., Raccanelli A., Riess A. G., 2016, Phys. Rev. Lett., 116, 201301
Breivik K., Rodriguez C. L., Larson S. L., Kalogera V., Rasio F. A., 2016, arXiv:1606.09558
Cutler C., 1998, Phys. Rev. D, 57, 7089
Cutler C., Vallisneri M., 2007, Phys. Rev. D, 76, 104018
Fairhurst S., 2009, New J. Phys., 11, 123006
Klein A. et al., 2016, Phys. Rev. D, 93, 024003
Kreidberg L., Bailyn C. D., Farr W. M., Kalogera V., 2012, Astrophys. J., 757, 36
Nishizawa A., Berti E., Klein A., Sesana A., 2016a, arXiv:1606.09295
Nishizawa A., Berti E., Klein A., Sesana A., 2016b, arXiv:1605.01341
Özel F., Psaltis D., Narayan R., McClintock J. E., 2010, Astrophys. J., 725, 1918
Postnov K. A., Yungelson L. R., 2014, Living Rev. Relativity, 17, 3
Rodriguez C. L., Haster C.-J., Chatterjee S., Kalogera V., Rasio F. A., 2016, Astrophys. J., 824, L8
Rodriguez C. L., Morscher M., Pattabiraman B., Chatterjee S., Haster C.-J., Rasio F. A., 2015, Phys. Rev. Lett, 115, 051101
Sasaki M., Suyama T., Tanaka T., Yokoyama S., 2016, Phys. Rev. Lett., 117, 061101
Schutz B. F., 1986, Nature, 323, 310
Schutz B. F., 2011, Classical Quantum Gravity, 28, 125023
Sesana A., 2016, Phys. Rev. Lett., 116, 231102
Seto N., 2004, Phys. Rev. D, 69, 123005
Seto N., 2014, Phys. Rev. D, 90, 027303
Seto N., 2016, Mon. Not. R. Astron. Soc., 460, L1
Takahashi R., Seto N., 2002, Astrophys. J., 575, 1030
Vecchio A., Wickham E. D. L., 2004, Phys. Rev. D, 70, 082002
Vitale S., 2016, Phys. Rev. Lett, 117, 051102